Synthetic Molecular Evolution of Pore-Forming Peptides by Iterative Combinatorial Library Screening

ARTICLE *in* ACS CHEMICAL BIOLOGY · FEBRUARY 2013

Impact Factor: 5.33 · DOI: 10.1021/cb300598k · Source: PubMed

5 AUTHORS, INCLUDING:

Aram Krauson
University of Pittsburgh
20 PUBLICATIONS **78** CITATIONS
SEE PROFILE

Jing He
Tulane University
38 PUBLICATIONS **141** CITATIONS
SEE PROFILE

Andrew R Hoffmann
Tulane University
5 PUBLICATIONS **31** CITATIONS
SEE PROFILE

ACS chemical biology

Articles

pubs.acs.org/acschemicalbiology

Synthetic Molecular Evolution of Pore-Forming Peptides by Iterative Combinatorial Library Screening

Aram J. Krauson,[†] Jing He,[†] Andrew W. Wimley, Andrew R. Hoffmann, and William C. Wimley*

Department of Biochemistry and Molecular Biology SL43, Tulane University School of Medicine, New Orleans, Louisiana 70112, United States

ABSTRACT: We previously reported the *de novo* design of a combinatorial peptide library that was subjected to high-throughput screening to identify membrane-permeabilizing antimicrobial peptides that have β-sheet-like secondary structure. Those peptides do not form discrete pores in membranes but instead partition into membrane interfaces and cause transient permeabilization by membrane disruption, but only when present at high concentration. In this work, we used a consensus sequence from that initial screen as a template to design an iterative, second generation library. In the 24−26-residue, 16,200-member second generation library we varied six residues. Two diad repeat motifs of alternating polar and nonpolar amino acids were preserved to maintain a propensity for non-helical secondary structure. We used a new high-throughput assay to identify members that self-assemble into equilibrium pores in synthetic lipid bilayers. This screen was done at a very stringent peptide to lipid ratio of 1:1000 where most known membrane-permeabilizing peptides, including the template peptide, are not active. In a screen of 10,000 library members we identified 16 (~0.2%) that are equilibrium pore-formers at this high stringency. These rare and highly active peptides, which share a common sequence motif, are as potent as the most active pore-forming peptides known. Furthermore, they are not α-helical, which makes them unusual, as most of the highly potent pore-forming peptides are amphipathic α-helices. Here we demonstrate that this synthetic molecular evolution-based approach, taken together with the new high-throughput tools we have developed, enables the identification, refinement, and optimization of unique membrane active peptides.

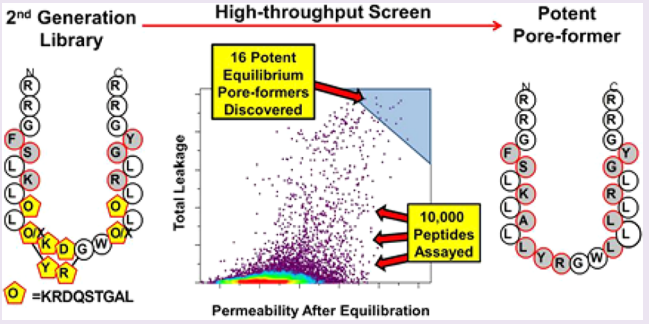

The ability to design peptides that self-assemble into equilibrium pores in membranes at very low peptide concentration could have utility in applications such as targetable cytotoxins,[1−4] chemo-sensitization agents,[5,6] exogenous ion channels,[7,8] or biosensor platforms.[9,10] While the basic architectural principles of peptide pore-formation at low concentration are understood, at least for α-helical pore-formers,[11,12] we do not yet have a molecular understanding of their mechanism of action. The lack of an explicit description of the sequence−structure−function relationships is a roadblock that prevents rational design and optimization for particular applications. The current "state of the art" in the field is limited to using one of the few naturally occurring peptides or to modifying known sequences by trial and error.[1−10] These approaches are further limited by the fact that most natural examples are amphipathic α-helices. Thus, we cannot currently design or optimize peptides with non-helical secondary structure that self-assemble into pores in membranes at low concentration.

Here, we are trying to identify such potent, equilibrium pore-forming peptides, which we define as peptides that (1) permeabilize lipid vesicles significantly at a peptide:lipid molar ratio of 1:1000 or less and (2) form pores in vesicles that are still present at equilibrium (i.e., a few hours after peptide addition). Importantly, these working definitions exclude most of the well-known membrane-permeabilizing antimicrobial peptides (e.g., cecropins, magainins, defensins, cathelicidins).[13−16] Even the archetypal "pore-forming peptide" melittin does not always satisfy these criteria.[17] Instead of forming potent, equilibrium pores, most antimicrobial peptides act by interfacial activity[13,18,19] against synthetic membranes, which means that (1) they are active in lipid vesicles only at high concentration (P:L > 1:50), (2) they are bound interfacially to membranes, and (3) they cause transient leakage through a pathway that is not detectable at equilibrium.[18,20−22] While there are many such interfacially active antimicrobial peptides described in the literature,[23] many with non-helical secondary structure, there are only a few known peptides that satisfy our working definition of potent, equilibrium pore-formers. Further limiting our knowledge, only a small number of these peptides have been studied in detail, and all of the well-studied examples (e.g., alamethicin) are amphipathic α-helices that share a similar architecture.

The lack of molecular understanding of potent, equilibrium pore-forming peptides is especially severe for non-helical ones because we have few, if any, natural examples. In the work

Received: November 4, 2012
Accepted: February 8, 2013
Published: February 8, 2013

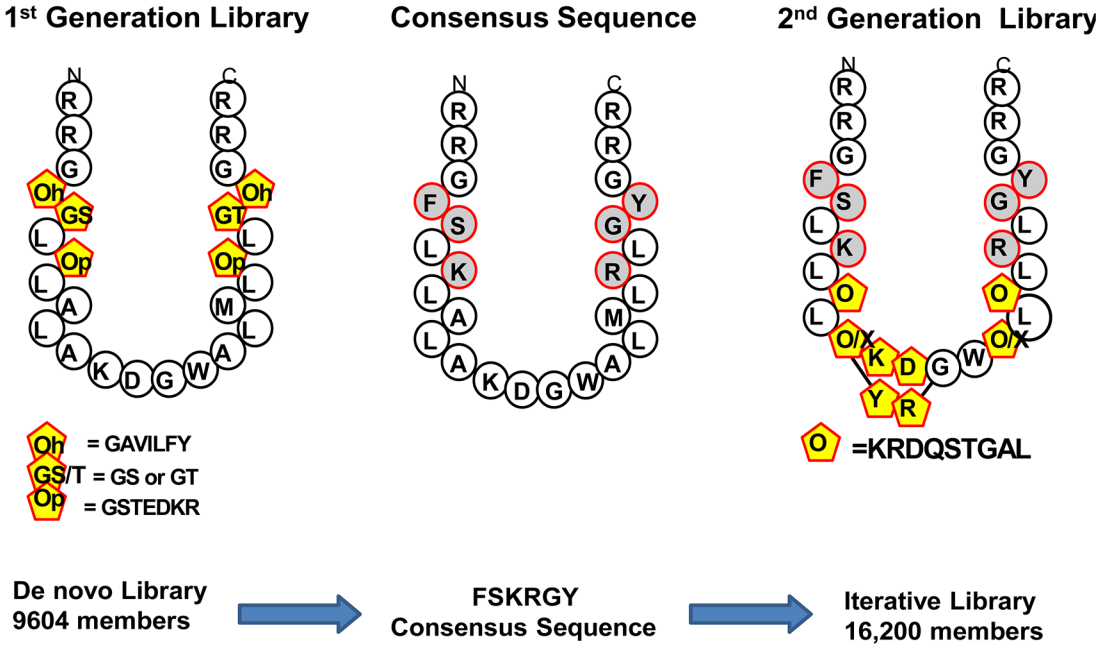

Figure 1. Iterative library design strategy. (Left) A *de novo* designed peptide library that was screened at low stringency for synthetic vesicle permeabilization.[27] The library is 26 residues long and biased to favor non-helical secondary structure.[28] Six residues were varied as shown in the figure by yellow shapes. From this library, a small number of active peptides were identified and characterized as we have described elsewhere.[27] (Right) To design the iterative library shown on the right we used an active sequence from the first library as a template (middle) and then varied six residues in positions near the linker segment between the two diad repeat motifs. In the variable positions, the library also contained members that had no residue (X), giving peptides between 24 and 26 residues. In addition to the four varied diad repeat positions (see text), we also allowed for the library to have either the original KD dipeptide or a more hydrophobic YR sequence. All peptides and libraries used are C-terminal amides.

presented here, we solve this problem by using a synthetic molecular evolution-based approach. This work is built upon our previous success in using lipid vesicle-based high-throughput screening to identify interfacially active[19,24−27] antimicrobial peptides with β-sheet-like secondary structure from *de novo* libraries.[19,28] For this work, we designed an iterative, second generation library based on an active consensus sequence from the first generation library in order to select at much higher stringency for potent, equilibrium pore formers. We describe how this synthetic molecular evolution approach successfully led to the discovery of potent, equilibrium pore-forming peptides that have non-helical, β-sheet-like secondary structure in membranes.

RESULTS AND DISCUSSION

Molecular Evolution of Pore-Forming Peptides. In this work, we set out to discover potent, equilibrium pore-forming peptides (as defined above) that have non-helical secondary structure in membranes. Although there are a very large number of membrane-permeabilizing peptides that have non-helical or β-sheet secondary structure,[23] such peptides are mostly interfacially active[18] antimicrobial peptides that permeabilize membranes only at high peptide concentration. Some well-studied examples include indolicidin,[29] protegrin,[30,31] tachyplesin,[32] lactoferricin,[33] and α,β- and Θ-defensins.[34,35] This class also includes FSKRGY and other families of non-helical peptides that we have discovered.[19,26] While it is possible that some of these peptides assemble into pore-like structures at high concentration, they are not sufficiently active to serve as precedents for the goals of this work.

The only examples of potent, equilibrium β-sheet pores are large oligomeric proteins such as α-hemolysin,[36,37] perfringolysin-O,[38] or the anthrax protective antigen.[39] These proteins insert a membrane-spanning β-barrel domain into membranes, supported by an oligomeric protein scaffold.[38,40] One of our long-term bioengineering goals is to design peptides that assemble into such membrane-spanning β-barrels at low concentration without a protein scaffold. Here we pursue an intermediate goal: the discovery of non-helical peptides that are highly potent, equilibrium pore-formers in membranes.

Iterative Library Design. We previously described a 26-residue, 9604-member combinatorial peptide library that was designed *de novo* to yield membrane-permeabilizing peptides that function by folding into β-sheets in membranes.[27,28] Upon screening this library for lipid vesicle permeabilization at a relatively low stringency of 1 peptide per 200 lipids (P:L = 1:200), we found that most members were inactive and that many of the inactive sequences were insoluble in aqueous solution. The most active (and soluble) ∼0.1% of the library members permeabilized lipid vesicles detectably but not with high potency. Nonetheless, we subsequently showed that these peptides, which contained a conserved compositional motif, are potent, broad-spectrum, biomembrane-permeabilizing antibiotics.[27,28] Like most antimicrobial peptides, the peptides identified in that screen permeabilize synthetic lipid membranes by a non-specific interfacial activity mechanism[18] and are active against synthetic bilayers only at high peptide concentrations[28] (P:L > 1:100).

Here we use an iterative library approach combined with high-throughput screening to identify potent, equilibrium, pore-forming peptides with non-helical secondary structure. Specifically, we used a maximally active consensus sequence from the first library as a template for designing a second, iterative library of about the same length. The 26-residue consensus sequence is named "FSKRGY" for the residues

dx.doi.org/10.1021/cb300598k | ACS Chem. Biol. 2013, 8, 823−831

found in the six varied positions. The two libraries and the consensus peptide, FSKRGY, that bridges them, are shown in Figure 1. In the iterative library we retained the overall architecture of FSKRGY, and we retained the specific residues that were selected in the initial screen that were near the termini of the sequence. In this second generation library we varied residues closer to the middle of the sequence (Figure 1). To favor non-helical secondary structure, the FSKRGY template sequence has two short diad repeats that are terminated by a stretch of four hydrophobes. In Figure 1, these sequence are **FSLK**<u>*L*</u>*ALA* on the N-terminal half and *ALM*<u>**L**</u>**RLGY** on the C-terminal half (the diad repeat is **bold** and the four hydrophobes are <u>underlined</u>). In this second generation library, we tested the idea that a more ideal diad repeat would favor potent pore formation by varying the two positions in the sequence that would extend the diad repeat (when the varied amino acid is polar). These positions are in *italic* above. Possible amino acids in these positions included hydrophobic, polar, and charged residues. The polar and charged residues not only allow for more ideal diad repeat motifs but also for cross-strand hydrogen bonds or salt bridges. They also allow for the possibility of a water-filled, transmembrane channel. The hydrophobic residues allow for deeper insertion into membranes and possible hydrophobic driven self-assembly.[41,42] We also included the possibility of having no amino acid in some of the positions (designated O/X in Figure 1), giving library members that vary in length between 24 and 26 residues. Finally we allowed for the replacement of the original lysine-aspartate (KD) in the connector region with a tyrosine-arginine (YR) sequence, which is expected to interact better with membranes.[43,44]

High-Throughput Screening. The iterative combinatorial library shown in Figure 1, which contains 16,200 members, was synthesized as a one bead−one sequence library, as described in detail elsewhere.[24−27,45] To determine the P:L ratio to be used in the high-throughput screen, we tested a sample of the iterative library and compared it to the original library at a low stringency of P:L = 1:200. The results, in Figure 2, show that the iterative strategy works; the second generation library is far more active than the original library, with a significant fraction

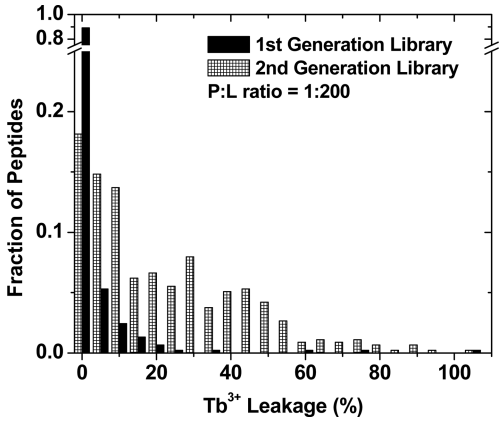

Figure 2. Comparison of the activity level in the initial library and the iterative library measured under identical conditions. In each case, several hundred randomly chosen library members were added to vesicles at a stringency of P:L = 1:200 using large unilamellar vesicles made from 90% POPC and 10% POPG. After incubation, leakage was measured, and the % leakage was calculated using the values for intact and detergent-lysed vesicles.

of members causing >20% leakage activity at P:L = 1:200, where the original library has very few active members. Note that only about 10% of the original library members have any measurable activity at all, whereas more than 80% of the second library members have measurable membrane-permeabilizing activity.

Based on the small scale test in Figure 2, we chose to screen the iterative, second generation library for potent activity and equilibrium pores at P:L = 1:1000 using the orthogonal *two step* assay, described below and elsewhere.[17,22] The *two step* assay measures leakage from vesicles (step one) and independently measures access to the vesicle interior through peptide pores after equilibration (step two). The second step is achieved by incubating samples for several hours after the addition of peptide to the vesicles and then adding dithionite $(S_2O_4)^{2-}$, a small molecule quencher of a lipid-linked NBD fluorophore. Only a potent, equilibrium pore-forming peptide will cause high leakage of Tb^{3+} at a stringency of 1:1000 and will also allow for high access of dithionite to the vesicle interior at equilibrium (which we define as a few hours after peptide addition).[17,22]

For screening, one dry photo-cleaved library bead (containing about 1 nmol of one peptide sequence) was placed in each well of a 96-well plate. The peptide was then extracted by incubating the bead overnight with 10 μL of dry dimethyl sulfoxide (DMSO) under vacuum. After extraction from the beads, peptides were pre-incubated in buffer in order to precipitate peptides with low aqueous solubility, thereby assuring that insoluble peptides will not show activity in the screen. A concentrated solution of liposomes was then added to achieve P:L = 1:1000. Vesicles were made from 90% zwitterionic phosphatidylcholine (PC) and 10% anionic phosphatidylglycerol (PG) as described below. After equilibration, the amount of Tb^{3+} leakage was measured, followed by NBD quenching[17,22] with dithionite to measure access to the vesicle interior. The cumulative results of the whole screen are shown in Figure 3. In panel A, we show a scatter plot of the leakage and NBD quenching for all 10,000 library members assayed in the high-throughput screen. In Panel B we show histograms of the two orthogonal measurements. Notice that at P:L = 1:1000 most library members (>99%) are inactive with leakage near zero. Similarly, the NBD quenching histogram is unimodal, with the peak of NBD quenching around 60%, which is due to the quenching of only the NBD lipids on the outer surface of the liposomes as observed with peptide-free control vesicles. At this stringency, very few library members cause leakage or create peptide-dependent access of the quencher to the vesicle interior.

In this work we focus on the few peptides that are soluble and form equilibrium pores at P:L = 1:1000, conditions under which the consensus peptide of the initial library, FSKRGY, is not active.[27,28] After screening 10,000 peptides at P:L = 1:1000 we found 16 (0.2%) exceptionally active, pore-forming peptides, with Tb^{3+} leakage greater than ∼90% and NBD quenching greater than ∼85%, indicative of a potent pore that remains active at equilibrium. This area of the cumulative plot (Figure 3A) is shown by the shaded triangular area in the upper right. The sequences of the active peptides were determined by Edman sequencing of the peptide that remains attached to the bead.

Potent Equilibrium Pore-Formers Identified. The sequences of the highly active peptides identified in the screen are given in Figure 4. Overall, they show a highly conserved composition, with hydrophobic residues predominantly se-

dx.doi.org/10.1021/cb300598k | *ACS Chem. Biol.* 2013, 8, 823−831

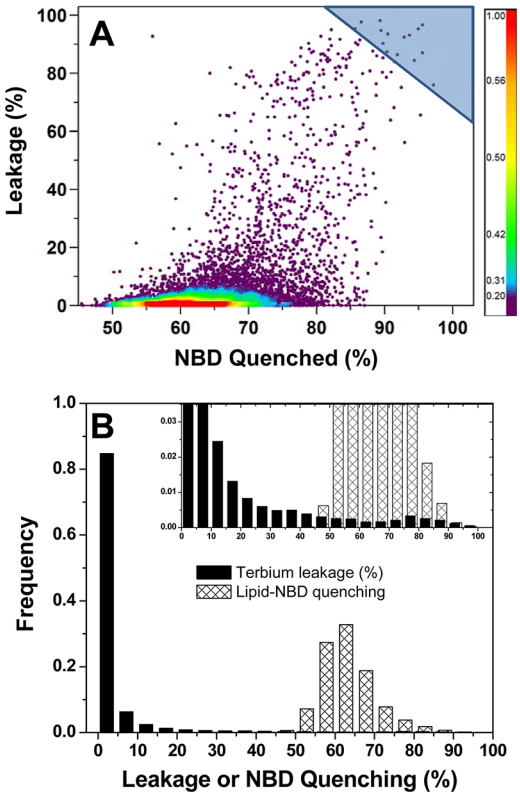

Figure 3. Results from the high-throughput screen of the iterative library. (A) *Two step* assay results for all 10,000 library members screened at P:L = 1:1000 using large unilamellar vesicles made from 90% POPC and 10% POPG. Each point is the result for one library member. Leakage (*y*-axis) is assessed by measuring the release of entrapped Tb^{3+} using external dipicolinic acid (step 1). Under these conditions, most library members are inactive with leakage near zero. Leakage ≥80% is very rare and indicates a very potent membrane-permeabilizing peptide. Quenching of NBD-lipids (*x*-axis) is assessed by adding the quencher dithionite at equilibrium (after hours-long incubation) and then measuring the degree of NBD-lipid quenching. In the presence of most library peptides, NBD quenching is near 60%, indicating that only surface-exposed lipids are quenched as expected for any vesicle. Quenching near 60% indicates that there is no access to the interior lipids (and thus no pores in the membrane). Quenching ≥90% indicates that dithionite can access the vesicle interior through equilibrium pores. A very small percentage of the 10,000 library members tested are active in both assays under these conditions. The area in the triangle at the upper right represents the most active peptides in the library with leakage and NBD-quenching at equilibrium greater than 90%. (B) Histograms of the data plotted in panel A shown with two different *y*-axis scales. These histograms show that most library members are inactive under these very stringent conditions. Highly active members are rare, accounting for 0.1% of the library.

lected in all of the combinatorial positions. The iteration peptides differ from the template FSKRGY by 3−6 residues, out of 26. Because of the very high similarity of the selected sequences to each other, we stopped the screening at 10,000 library members to focus on characterization of the motif. In the selected peptides, there was a very high proportion of hydrophobic amino acids and a correspondingly low proportion of the possible polar/charged amino acids. Out of 64 varied positions 46 contained either leucine (L), alanine (A), or glycine (G), including 27 that had leucine. This is compared to only 9 total instances of the polar residues serine (S), threonine (T), arginine (R), and lysine (K), and no instances of glutamine (Q) or aspartate (D). The *p*-value for such a favored selection of hydrophobes over polar residues is less than 0.0001. The preferential selection of hydrophobes was more stringent in the C-terminal sites, where every varied residue was either leucine, alanine, or glycine. In the N-terminal varied sites, there was more variability, especially at position 9, which was found to contain a few instances of serine, threonine, lysine, and arginine along with the hydrophobes. The variable loop residues, which were either the original zwitterionic lysine-aspartate (KD) or cationic tyrosine-arginine (YR), showed a possible preference for YR (11/16) over KD, perhaps because YR interacts better with membranes.[46,47] Interestingly, the more polar KD sequence was associated with more hydrophobic residues in the other sites (see Figure 4), while the less polar YR sequence was associated with the less hydrophobic residues overall, supporting the idea that a key selection feature is the overall hydrophobicity.

In the combinatorial library, the peptide length varied between 24 and 26 residues because two of the combinatorial sites also had no amino acid (X) as a library variation. In the highly active peptides, we found 25- and 26-residue peptides. All of the observed variations in length occurred due to a missing residue in the C-terminal combinatorial site. In every case where a shorter 25-residue peptide was found (which was about half of the time) the nearby varied residue was leucine. Thus the shortened sequences appear to only be found when the overall sequence nearby can maintain its very hydrophobic nature.

Pore-Forming Activity. To characterize the selected pore-formers, we synthesized and purified FSKRGY and the six peptides shown in Figure 5. The peptide It−1c is a consensus sequence based on the observed variants but was not actually observed in the screen. The other five peptides were observed in the screen. FSKRGY, the template peptide for the iterative library, causes significant membrane permeabilization only at P:L ratios of 1:100 or larger.[27,28] Furthermore, we have shown that the leakage induced by FSKRGY is a transient event that occurs only in the first 15−30 min after peptide addition.[28] The iteration peptides selected from the second generation library are far more active; they permeabilize 90:10 PC:PG vesicles at P:L ≤ 1:1000 or lower and remain active in membranes at equilibrium (i.e., hours after peptide addition) as shown in Figure 3.

To test the robustness and generality of the observed activity, we next measured the membrane-permeabilizing activity of these peptides in a variety of lipid compositions, using a different leakage indicator system. Measurements such as these are needed to demonstrate that we did not select for a pore-forming activity that was highly dependent on the details of the screening assay. Also, in these experiments, we measured leakage after 3 h to eliminate the effect of slow processes we might have selected for in the overnight high-throughput screen. Vesicles of five different lipid compositions, containing the entrapped fluorophore ANTS and its obligate quencher DPX, were used to test the effect of membrane physical properties in pore-forming peptide activity. Despite the significant differences in buffer, leakage probe, and incubation time, the results in Figure 6 show that the selected peptides have much higher activity than FSKRGY in 90:10 PC:PG vesicles that were used in the screen and also in pure PC vesicles without PG. The iteration peptides are 5−20-fold more active (i.e., there is a 5−20-fold decrease in the peptide concentration required to cause 50% leakage). It is interesting

dx.doi.org/10.1021/cb300598k | *ACS Chem. Biol.* 2013, 8, 823−831

R	R	G	F	S	L	K	L	O	L	O X	KD YR	G	W	O X	L	O	L	R	L	G	Y	G	R	R
1	2	3	4	5	6	7	8	9	10	11	12	13	14	15	16	17	18	19	20	21	22	23	24	25	26

Library Sequence (O= KRDQSTGAL)

Screening Results

R	R	G	F	S	L	K	L	A	L	L	K	D	G	W	L	L	L	L	R	L	G	Y	G	R	R
R	R	G	F	S	L	K	L	A	L	L	K	D	G	W	L	L	L	L	R	L	G	Y	G	R	R
R	R	G	F	S	L	K	L	A	L	L	K	D	G	W	L	L	L	L	R	L	G	Y	G	R	R
R	R	G	F	S	L	K	L	A	L	L	K	D	G	W	X	L	L	L	R	L	G	Y	G	R	R
R	R	G	F	S	L	K	L	A	L	L	Y	R	G	W	X	L	A	L	R	L	G	Y	G	R	R
R	R	G	F	S	L	K	L	L	L	A	Y	R	G	W	A	X	L	L	R	L	G	Y	G	R	R
R	R	G	F	S	L	K	L	L	L	S	Y	R	G	W	A	X	L	L	R	L	G	Y	G	R	R
R	R	G	F	S	L	K	L	L	L	S	Y	R	G	W	X	L	L	L	R	L	G	Y	G	R	R
R	R	G	F	S	L	K	L	L	L	T	Y	R	G	W	L	L	L	L	R	L	G	Y	G	R	R
R	R	G	F	S	L	K	L	G	L	G	Y	R	G	W	X	L	L	L	R	L	G	Y	G	R	R
R	R	G	F	S	L	K	L	G	L	T	Y	R	?	?	?	?	?								
R	R	G	F	S	L	K	L	T	L	A	Y	R	G	W	X	L	L	L	R	L	G	Y	G	R	R
R	R	G	F	S	L	K	L	S	L	L	Y	R	G	W	X	L	L	L	R	L	G	Y	G	R	R
R	R	G	F	S	L	K	L	R	L	L	Y	R	G	W	G	L	A	L	R	L	G	Y	G	R	R
R	R	G	F	S	L	K	L	R	L	L	K	D	G	W	A	L	A	L	R	L	G	Y	G	R	R
R	R	G	F	S	L	K	L	K	L	L	Y	R	G	W	A	L	A	L	R	L	G	Y	G	R	R

									# observed total	P=value overall
L	4		9	KD=5		4		11	28 L	P<0.001
A	5		2			4		4	15 A	P=0.02
G	2		1	YR=11		1		0	4 G	P=0.04
S	1		2			0		0	3 S	P=0.04
T	1		2			0		0	3 T	P=0.01
R	2		0			0		0	2 R	P=0.01
K	1		0			0		0	1 K	P=0.003
D	0		0			0		0	0 D	P<0.001
Q	0		0			0		0	0 Q	P<0.001
X			0			8			8X	
									47 LAG 9 STRK 0 QD	P<0.0001

Figure 4. Sequences of 16 highly active iterative library members identified in the high-throughput screen. The sequence of the template peptide FSKRGY and of the iterative library are also shown in Figure 1. The sequences of the most active iteration peptides are shown here arranged from the most hydrophobic to the most polar, top to bottom. The varied residues in the two diad repeat segments are shown in green, and the "turn" residues are shown in orange. *P*-values represent the probability that the observed abundance of residues was obtained strictly by chance, as calculated using the expected binomial statistics.[26] "X" means that the sequence had no residue at that position. "?" means that a sequencer malfunction occurred and the residues were not identified.

to note that the consensus sequence It−1c is remarkably active against PC vesicles even when compared to the selected peptides. We speculate that this activity is related to its higher secondary structure content (see below), but that it was not selected in the screen because it is less soluble.

The pore-forming activity of these peptides is surprisingly sensitive to the lipid composition. First, compared to the activity in PC:PG vesicles in which they were selected, all of the peptides are generally less active (higher LIC_{50}) in bilayers made from other lipids, except for PC. For example, in bilayers made from 60% PC with 30% zwitterionic phosphatidylethanolamine (PE) and 10% anionic phosphatidylserine (PS) the peptides are less active, overall. However, in these bilayers the iteration peptides are still 2−4-fold more active than FSKRGY. In pure anionic PG bilayers, the template sequence FSKRGY and the iteration sequences have similarly low activity and there is little difference between them. Perhaps most interestingly, in PC bilayers with 25% cholesterol, activity of all the peptides is very low and there is essentially no difference between the activity of FSKRGY and the iteration peptides. We speculate that the increased rigidity of cholesterol-containing bilayers inhibits the folding and self-assembly of the peptides.

Folding and Secondary Structure. Circular dichroism spectroscopy was used to assess the secondary structure of the peptides in solution and in lipid bilayers. CD experiments were done in the absence and presence of 1 mM 90:10 PC:PG vesicles. Under these conditions all of the peptides are more than 85% bound to bilayers[21,28] such that the spectra report

dx.doi.org/10.1021/cb300598k | *ACS Chem. Biol.* 2013, 8, 823−831

FSKRGY	R	R	G	F	S	L	K	L	A	L	A	K	D	G	W	A	L	M	L	R	L	G	Y	G	R	R	26	+7
It–1a	R	R	G	F	S	L	K	L	L	L	S	Y	R	G	W	A	_	L	L	R	L	G	Y	G	R	R	25	+8
It–1b	R	R	G	F	S	L	K	L	A	L	L	K	D	G	W	_	L	L	L	R	L	G	Y	G	R	R	25	+7
It–1c**	R	R	G	F	S	L	K	L	A	L	L	Y	R	G	W	L	L	L	L	R	L	G	Y	G	R	R	26	+8
It–1d	R	R	G	F	S	L	K	L	R	L	L	Y	R	G	W	G	L	A	L	R	L	G	Y	G	R	R	26	+9
It–1e	R	R	G	F	S	L	K	L	K	L	L	Y	R	G	W	A	L	A	L	R	L	G	Y	G	R	R	26	+9
It–1f	R	R	G	F	S	L	K	L	A	L	L	K	D	G	W	L	L	L	L	R	L	G	Y	G	R	R	26	+7

Figure 5. Sequences of the peptides synthesized for further study. Residues that were varied in the library are shaded as in Figure 4; the two diad repeat segments are shown in green, and the "turn" residues are shown in orange. FSKRGY is the 26-residue template sequence, identified in an earlier library[27,28] and used as a template for the iteration library screened here. The active peptides from the iteration library are named It−1 peptides. **It−1c is a consensus sequence that was not actually observed in the screen. The others sequences were actually observed in the screen. The number of residues and the total charge are shown on the right.

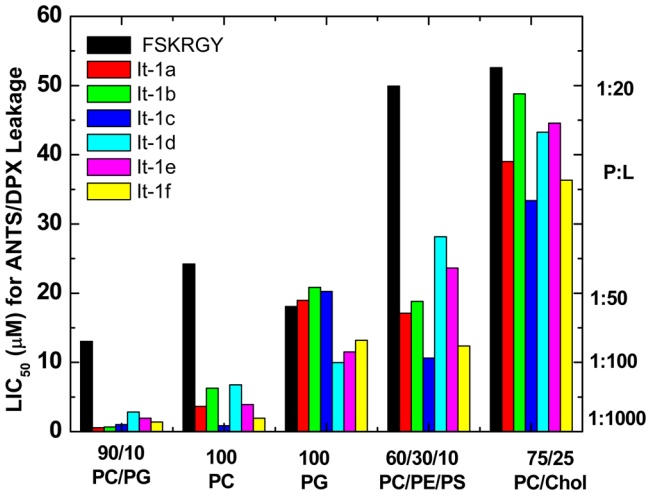

Figure 6. Membrane permeabilization by template peptide, FSKRGY, and by the iteration peptides It−1a through It−1f. Leakage of ANTS/DPX was measured by fluorescence.[56] In this experiment we used vesicles made from various lipid compositions at 1 mM lipid and measured the amount of leakage at 3 h after the addition of peptides at various concentration. The leakage curves were hyperbolic or sigmoidal.[18] The peptide concentration that induces 50% leakage (LIC_{50} or leakage-inducing concentration of 50%) was obtained by curve fitting.

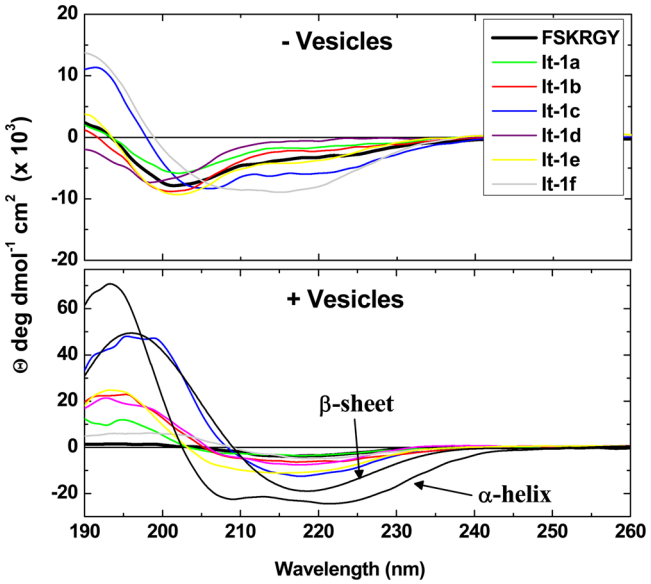

Figure 7. Circular dichroism spectroscopy. Aliquots of peptide in distilled water were diluted into buffer to achieve 25 μM peptide. (Top) CD spectra for peptides in buffer only. (Bottom) Peptides in buffer containing 1 mM large unilamellar vesicles of 90% POPC and 10% POPG. Samples were incubated at least a few hours prior to data collection. Spectra are converted to mean residue ellipticity. In the bottom panel we show, for comparison, the CD spectra for a fully α-helical melittin analogue[17] in membranes and for a highly organized, membrane inserted antiparallel β-sheet peptide.[42,48]

mostly on the membrane bound form. The CD results, in Figure 7 show that FSKRGY and the iteration peptides are mostly random coil in buffer, as indicated by the minimum in their CD spectra around 200 nm. The exceptions are It−1c and It−1f, which have a small amount of secondary structure in solution, as shown by the negative ellipticity at 210−225 nm and a positive ellipticity at 200 nm.

In bilayers, all of the pore-forming peptides gain secondary structure, as shown by a positive ellipticity at ∼200 and a broad band of negative ellipticity centered at 218 nm. For comparison, we show the CD spectra for a membrane-bound α-helical peptide (an analogue of melittin[17]) and for a membrane-bound, antiparallel β-sheet peptide,[48] $AcWL_5$. Although the secondary structure of the peptides discovered here is not very well-defined by the CD spectra, the peptides are clearly not α-helical in membranes. The minimum in ellipticity at 218 nm suggests that the secondary structure is composed of mostly β-sheet-like structure; however, the minimum is broad and relatively weak, suggesting that the secondary structure is not homogeneous or highly ordered. The peptide $AcWL_5$, shown in the figure for comparison, forms very highly ordered antiparallel β-sheets in membranes (verified by one-dimensional and two-dimensional FTIR[48,49]). The CD spectra for these iteration peptides in bilayers are very similar to β-sheet-rich soluble proteins[50] and are thus also similar to β-sheet basis spectra used in soluble protein structure deconvolution.[51] While these CD spectra were collected at P:L that was higher than for the leakage experiments, we observed no concentration dependence of CD spectra down to concentrations as low as P:L = 1:1000, and therefore the spectra presented are relevant to the functional assays.

Mean residue ellipticities of protein and peptide β-sheets are variable, with values of +20−60,000 deg $dmol^{-1}$ cm^2 at 200 nm and values of −5 to −20,000 deg $dmol^{-1}$ cm^2 at 218 nm.[42,48,52−54] On the basis of the observed ellipticities for the iteration peptides in Figure 7, we conclude that some of the iteration peptides could contain up to 50% β-sheet and that FSKRGY contains much less secondary structure than the iteration peptides. Interestingly, the consensus sequence of It−

dx.doi.org/10.1021/cb300598k | ACS Chem. Biol. 2013, 8, 823−831

1c, which was present in the library but not selected, is much more structured in bilayers than the sequences that were actually selected. We suggest that the lack of selection of It−1c was the result of our pre-selection for peptide solubility, which would be expected to eliminate peptides with a secondary structure propensity that is too high. However, we also note that we arrived at a consensus composition after screening only a portion of the library, and so it remains possible that It−1c would have been identified in screen that sampled 100% of the library.

Insight into the Mechanism of Pore-Formation. In a recent electrochemical impedance spectroscopy (EIS) study[21] using supported bilayers we compared FSKRGY and a peptide that was referred to as FSKRGY-L3, which is the same peptide as It−1b in this paper. A comparison of the two studies gives insight into the mechanism of membrane permeabilization. Impedance spectroscopy is very sensitive to small changes in bilayer resistance resulting from increased passage of small ions such as H^+, Na^+, and Cl^-. On the other hand, vesicle leakage requires the cooperative action of multiple peptides in order to release much larger analytes. By impedance spectroscopy we observed a significant decrease in membrane resistance due to FSKRGY concentrations as low as 1 peptide per 40,000 lipids, a concentration that is almost 3 orders of magnitude lower than the peptide to lipid ratio of ∼1:50 that is required for significant vesicle leakage by FSKRGY. This suggests that monomeric FSKRGY causes defects in bilayer packing that can be detected by impedance but does not act cooperatively in vesicles to release larger analytes until its concentration in the bilayer is much higher. By impedance, It−1b also causes defects in bilayers at low concentration, at P:L = 1:10,000, suggesting that the iteration peptides interact with membranes at very low concentration in a way that is similar to FSKRGY. This conclusion is reasonable considering that the length, sequence, and hydrophobicity of the two peptides are similar. However, in contrast to the impedance experiments, vesicle leakage assays show a very large difference in the relative activities of FSKRGY and It−1b. For example, It−1b causes vesicle leakage at P:L = 1:1000, whereas FSKRGY requires P:L = 1:50 or higher to cause probe leakage in the same vesicles. Taken together, this comparison of techniques suggests that the major difference between FSKRGY and the iteration peptides is not their basic mode of interaction with membranes, but rather their propensity to self-assemble. Experiments designed to test this hypothesis by exploring the structure-function relationships of these peptides are underway.

Conclusions. In the work presented here, we have used a novel iterative library design and high-throughput screening strategy as a form of synthetic molecular evolution to identify extremely potent, equilibrium pore-forming peptides. We were successful after just two "generations" of small libraries and presumably will be able to increase activity further with additional generations. This is the first time such an approach has been used to design, *de novo*, any class of pore-forming peptide. Furthermore, the peptides identified in this screen were successfully designed to have non-helical, β-sheet-like secondary structure, which is essentially unknown among the few peptides that form pores in membranes at low concentration. With the methods described here, we have enabled the design, engineering and optimization of potent, membrane-selective, pore-forming peptides for many potential applications. This successful application of synthetic molecular evolution may have broad applicability for understanding, and for engineering, the structure−function relationships of peptides with activity in biomembranes.

METHODS

Combinatorial Peptide Library Synthesis. The iterative combinatorial peptide library was synthesized on Tentagel NH_2 macrobeads (300 mm diameter) as described in detail elsewhere.[24,26,27,45] Validation of library synthesis was done using mass spectrometry, HPLC, and Edman sequencing. The photocleavable linker attaching the peptide to the bead was cleaved with 5 h of low power UV light on dry beads spread to a sparse single layer in a glass dish. The beads released an average of 0.5 nmol per bead, which is about 1/3 of the total peptide on the bead. Edman sequencing was performed directly using the peptide that remains covalently attached to the beads.

***Two Step* Assay.** Unilamellar vesicles of 0.1 μm diameter were made by extrusion[55] from 90% 1-palmitoyl-2-oleoyl-*sn*-3-glycero-phosphocholine (POPC), 10% 1-palmitoyl-2-oleoyl-*sn*-3-glycero-phosphoglycerol (POPG), and 0.1% NBD-headgroup-labeled phospholipids. The vesicles also contained entrapped terbium and external dipicolinic acid for measurement of leakage.[17,22,24,26,27] To use the *two step* assay in high-throughput screens, each peptide was present in the well of a 96-well plate at about 1 μM and lipid concentration was 1 mM to achieve P:L = 1:1000. Wells with only liposomes were used as negative controls, and wells with liposomes plus 0.1% (final concentration) reduced Triton-X 100 detergent were used as positive controls. In most samples, peptide-induced leakage occurs within 30 min; however, we wanted to measure NBD quenching at equilibrium, and thus samples were incubated for at least 8 h. Terbium leakage was measured, followed by NBD-quenching with dithionite.[17,22] All measurements were made using a Biotek Synergy plate reader. Sensitivity was adjusted so that the detergent-lysed positive controls' arbitrary fluorescence was roughly 30% of the instrument maximum. To assess the accessibility to the interior of the vesicles at equilibrium in the same 96-well plate samples, we measured the quenching of NBD fluorescence as a function of time following the addition of 25 μM dithionite from a freshly prepared concentrated stock solution of 0.6 M in pH 10 buffer.[17,22]

For high-throughput screens, library beads with dry-cleaved photolinker were placed into the wells of a 96-well plate. Ten microliters (10 μL) of DMSO was added to each well, and the plate was placed under vacuum overnight to extract the peptide from the bead. After vacuum-extraction, 110 μL of buffer was added into each well, and the plate was allowed to incubate for at least 4 h to allow for precipitation of insoluble peptides. One hundred twenty microliters (120 μL) of 2 mM liposomes with 1 mol % NBD-labeled lipids was added. The final peptide to lipid ratio (P:L) was ∼1:1,000. Plates were stored at −20 C for selected beads to be sequenced.

ANTS/DPX Leakage. ANTS at 5 mM and DPX at 12.5 mM in 10 mM sodium phosphate buffer were entrapped in 0.1 μm diameter extruded vesicles with various lipid compositions as described elsewhere.[17,56] All lipids were 1-palmitoyl-2-oleoyl-*sn*-3-glycero-phospholipids, except for cholesterol. The external buffer was 10 mM sodium phosphate, 40 mM NaCl, pH 7.0. Leakage was quantitated by the increase in ANTS fluorescence that occurs when the entrapped DPX quencher is diluted into the external buffer upon permeabilization. ANTS/DPX containing vesicles[56] were diluted to 1 mM total lipid concentration, and peptide was added at concentrations between 0.5 and 20 μM, giving P:L between 0.0005 (1:2000) and 0.02 (1:50). Leakage was measured after 3 h incubation. The concentration dependence of leakage was fit with a hyperbolic/sigmoidal curve, and the peptide concentration that causes 50% leakage (LIC_{50}) was determined from the curve fits.

Circular Dichroism. Spectroscopic measurements were performed as described elsewhere.[26,28] Briefly, peptide was dissolved in buffer (10 mM sodium phosphate, 40 mM NaCl, pH 7.0) and also at the same concentration in buffer containing 1 mM 90:10 PC:PG large unilamellar vesicles. A concentration of 25 μM peptide was used for circular dichroism. After incubation for several hours at RT (to ensure

equilibrium), circular dichroism spectra were collected in a 1 mm × 10 mm rectangular quartz cuvette in a JASCO 810 spectropolarimeter.

AUTHOR INFORMATION

Corresponding Author

*E-mail: wwimley@tulane.edu.

Author Contributions

†These authors contributed equally to this work.

Notes

The authors declare no competing financial interest.

ACKNOWLEDGMENTS

We appreciate the contributions of T. Freeman for data analysis software. Funded by National Institutes of Health grant GM060000 and NSF grant DMR-1003411.

REFERENCES

(1) Pan, H, Soman, N. R., Schlesinger, P. H., Lanza, G. M., and Wickline, S. A. (2011) Cytolytic peptide nanoparticles ('NanoBees') for cancer therapy. *Interdiscip. Rev. Nanomed. Nanobiotechnol. 3*, 318−27.

(2) Soman, N. R., Baldwin, S. L., Hu, G., Marsh, J. N., Lanza, G. M., Heuser, J. E., Arbeit, J. M., Wickline, S. A., and Schlesinger, P. H. (2009) Molecularly targeted nanocarriers deliver the cytolytic peptide melittin specifically to tumor cells in mice, reducing tumor growth. *J. Clin. Invest. 119*, 2830−42.

(3) Holle, L., Song, W., Holle, E., Wei, Y., Li, J., Wagner, T. E., and Yu, X. (2009) In vitro- and in vivo-targeted tumor lysis by an MMP2 cleavable melittin-LAP fusion protein. *Int. J. Oncol. 35*, 829−35.

(4) Jo, M., Park, M. H., Kollipara, P. S., An, B. J., Song, H. S., Han, S. B., Kim, J. H., Song, M. J., and Hong, J. T. (2012) Anti-cancer effect of bee venom toxin and melittin in ovarian cancer cells through induction of death receptors and inhibition of JAK2/STAT3 pathway. *Toxicol. Appl. Pharmacol. 258*, 72−81.

(5) Gerlach, S. L., Rathinakumar, R., Chakravarty, G., Goransson, U., Wimley, W. C., Darwin, S. P., and Mondal, D. (2010) Anticancer and chemosensitizing abilities of cycloviolacin 02 from Viola odorata and psyle cyclotides from Psychotria leptothyrsa. *Biopolymers 94*, 617−25.

(6) Muller-Schiffmann, A., Sticht, H., and Korth, C. (2012) Hybrid compounds: from simple combinations to nanomachines. *BioDrugs 26*, 21−31.

(7) Wallace, D. P., Tomich, J. M., Eppler, J. W., Iwamoto, T., Grantham, J. J., and Sullivan, L. P. (2000) A synthetic channel-forming peptide induces Cl(-) secretion: modulation by Ca(2+)-dependent K(+) channels. *Biochim. Biophys. Acta 1464*, 69−82.

(8) Mitchell, K. E., Iwamoto, T., Tomich, J., and Freeman, L. C. (2000) A synthetic peptide based on a glycine-gated chloride channel induces a novel chloride conductance in isolated epithelial cells. *Biochim. Biophys. Acta 1466*, 47−60.

(9) Majd, S., Yusko, E. C., Billeh, Y. N., Macrae, M. X., Yang, J., and Mayer, M. (2010) Applications of biological pores in nanomedicine, sensing, and nanoelectronics. *Curr. Opin. Biotechnol. 21*, 439−76.

(10) Sexton, L. T., Horne, L. P., and Martin, C. R. (2007) Developing synthetic conical nanopores for biosensing applications. *Mol. Biosyst. 3*, 667−85.

(11) Leitgeb, B., Szekeres, A., Manczinger, L., Vagvolgyi, C., and Kredics, L. (2007) The history of alamethicin: a review of the most extensively studied peptaibol. *Chem. Biodivers. 4*, 1027−51.

(12) Bechinger, B. (1997) Structure and functions of channel-forming peptides: Magainins, cecropins, melittin and alamethicin. *J. Membr. Biol. 156*, 197−211.

(13) Wimley, W. C., and Hristova, K. (2011) Antimicrobial peptides: Successes, challenges and unanswered questions. *J. Membr. Biol. 239*, 27−34.

(14) Hancock, R. E., and Sahl, H. G. (2006) Antimicrobial and host-defense peptides as new anti-infective therapeutic strategies. *Nat. Biotechnol. 24*, 1551−7.

(15) Jenssen, H., Hamill, P., and Hancock, R. E. (2006) Peptide antimicrobial agents. *Clin. Microbiol. Rev. 19*, 491−511.

(16) Yount, N. Y., Bayer, A. S., Xiong, Y. Q., and Yeaman, M. R. (2006) Advances in antimicrobial peptide immunobiology. *Biopolymers 84*, 435−58.

(17) Krauson, A. J., He, J., and Wimley, W. C. (2012) Gain-of-function analogues of the pore-forming peptide melittin selected by orthogonal high-throughput screening. *J. Am. Chem. Soc. 134*, 12732−41.

(18) Wimley, W. C. (2010) Describing the mechanism of antimicrobial peptide action with the interfacial activity model. *ACS Chem. Biol. 5*, 905−17.

(19) Rathinakumar, R., Walkenhorst, W. F., and Wimley, W. C. (2009) Broad-spectrum antimicrobial peptides by rational combinatorial design and high-throughput screening: The importance of interfacial activity. *J. Am. Chem. Soc. 131*, 7609−17.

(20) Shai, Y., and Oren, Z. (2001) From "carpet" mechanism to de-novo designed diastereomeric cell-selective antimicrobial peptides. *Peptides 22*, 1629−41.

(21) Lin, J., Motylinski, J., Krauson, A. J., Wimley, W. C., Searson, P. C., and Hristova, K. (2012) Interactions of membrane active peptides with planar supported bilayers: an impedance spectroscopy study. *Langmuir 28*, 6088−96.

(22) Krauson, A. J., He, J., and Wimley, W. C. (2012) Determining the mechanism of membrane permeabilizing peptides: Identification of potent, equilibrium pore-formers. *Biochim. Biophys. Acta 1818*, 1625−32.

(23) Fjell, C. D., Hancock, R. E., and Cherkasov, A. (2007) AMPer: A database and an automated discovery tool for antimicrobial peptides. *Bioinformatics 23*, 1148−55.

(24) Marks, J. R., Placone, J., Hristova, K., and Wimley, W. C. (2011) Spontaneous membrane-translocating peptides by orthogonal high-throughput screening. *J. Am. Chem. Soc. 133*, 8995−9004.

(25) Rathinakumar, R., and Wimley, W. C. (2010) High-throughput discovery of broad-spectrum peptide antibiotics. *FASEB J. 24*, 3232−8.

(26) Rathinakumar, R., and Wimley, W. C. (2008) Biomolecular engineering by combinatorial design and high-throughput screening: small, soluble peptides that permeabilize membranes. *J. Am. Chem. Soc. 130*, 9849−58.

(27) Rausch, J. M., Marks, J. R., and Wimley, W. C. (2005) Rational combinatorial design of pore-forming β-sheet peptides. *Proc. Natl. Acad. Sci. U.S.A. 102*, 10511−5.

(28) Rausch, J. M., Marks, J. R., Rathinakumar, R., and Wimley, W. C. (2007) β-sheet pore-forming peptides selected from a rational combinatorial library: mechanism of pore formation in lipid vesicles and activity in biological membranes. *Biochemistry 46*, 12124−39.

(29) Rozek, A., Friedrich, C. L., and Hancock, R. E. (2000) Structure of the bovine antimicrobial peptide indolicidin bound to dodecylphosphocholine and sodium dodecyl sulfate micelles. *Biochemistry 39*, 15765−74.

(30) Mani, R., Buffy, J. J., Waring, A. J., Lehrer, R. I., and Hong, M. (2004) Solid-state NMR investigation of the selective disruption of lipid membranes by protegrin-1. *Biochemistry 43*, 13839−48.

(31) Su, Y., Waring, A. J., Ruchala, P., and Hong, M. (2011) Structures of β-hairpin antimicrobial protegrin peptides in lipopolysaccharide membranes: mechanism of gram selectivity obtained from solid-state nuclear magnetic resonance. *Biochemistry 50*, 2072−83.

(32) Kawano, K., Yoneya, T., Miyata, T., Yoshikawa, K., Tokunaga, F., Terada, Y., and Iwanaga, S. (1990) Antimicrobial peptide, tachyplesin I, isolated from hemocytes of the horseshoe crab (Tachypleus tridentatus). NMR determination of the β-sheet structure. *J. Biol. Chem. 265*, 15365−7.

(33) Schibli, D. J., Hwang, P. M., and Vogel, H. J. (1999) The structure of the antimicrobial active center of lactoferricin B bound to sodium dodecyl sulfate micelles. *FEBS Lett. 446*, 213−7.

(34) White, S. H., Wimley, W. C., and Selsted, M. E. (1995) Structure, function, and membrane integration of defensins. *Cur. Opinion Struct. Biol. 5*, 521−7.

(35) Wimley, W. C., Selsted, M. E., and White, S. H. (1994) Interactions between human defensins and lipid bilayers: Evidence for the formation of multimeric pores. *Protein Sci. 3*, 1362−73.
(36) Montoya, M., and Gouaux, E. (2003) β-Barrel membrane protein folding and structure viewed through the lens of α-hemolysin. *Biochim. Biophys. Acta 1609*, 19−27.
(37) Gouaux, E. (1998) α-Hemolysin from *Staphylococcus aureus*: An archetype of β-barrel, channel-forming toxins. *J. Struct. Biol. 121*, 110−22.
(38) Ramachandran, R., Heuck, A. P., Tweten, R. K., and Johnson, A. E. (2002) Structural insights into the membrane-anchoring mechanism of a cholesterol-dependent cytolysin. *Nat. Struct. Biol. 9*, 823−7.
(39) Petosa, C., Collier, R. J., Klimpel, K. R., Leppla, S. H., and Liddington, R. C. (1997) Crystal structure of the anthrax toxin protective antigen. *Nature (London) 385*, 833−8.
(40) Heuck, A. P., and Johnson, A. E. (2002) Pore-forming protein structure analysis in membranes using multiple independent fluorescence techniques. *Cell Biochem. Biophys. 36*, 89−101.
(41) Han, X., Hristova, K., and Wimley, W. C. (2008) Protein folding in membranes: insights from neutron diffraction studies of a membrane β-sheet oligomer. *Biophys. J. 94*, 492−505.
(42) Bishop, C. M., and Wimley, W. C. (2011) Structural plasticity in self-assembling transmembrane β-sheets. *Biophys. J. 101*, 828−36.
(43) White, S. H., and Wimley, W. C. (1999) Membrane protein folding and stability: physical principles. *Annu. Rev. Biophys. Biomol. Struct. 28*, 319−65.
(44) White, S. H., and Wimley, W. C. (1998) Hydrophobic interactions of peptides with membrane interfaces. *Biochim. Biophys. Acta 1376*, 339−52.
(45) He, L., Hoffmann, A. R., Serrano, C., Hristova, K., and Wimley, W. C. (2011) High-throughput selection of transmembrane sequences that enhance receptor tyrosine kinase activation. *J. Mol. Biol. 412*, 43−54.
(46) Wimley, W. C., and White, S. H. (1996) Experimentally determined hydrophobicity scale for proteins at membrane interfaces. *Nat. Struct. Biol. 3*, 842−8.
(47) Hristova, K., and Wimley, W. C. (2010) A look at arginine in membranes. *J. Membr. Biol. 239*, 49−56.
(48) Wimley, W. C., Hristova, K., Ladokhin, A. S., Silvestro, L., Axelsen, P. H., and White, S. H. (1998) Folding of β-sheet membrane proteins: A hydrophobic hexapeptide model. *J. Mol. Biol. 277*, 1091−110.
(49) Paul, C., Wang, J., Wimley, W. C., Hochstrasser, R. M., and Axelsen, P. H. (2004) Vibrational coupling, isotopic editing, and β-sheet structure in a membrane-bound polypeptide. *J. Am. Chem. Soc. 126*, 5843−50.
(50) Johnson, W. C. (1990) Protein secondary structure and circular dichroism: A practical guide. *Proteins 7*, 205−14.
(51) Johnson, W. C. (1988) Secondary structure of proteins through circular dichroism spectroscopy. *Annu. Rev. Biophys. Biophys. Chem. 17*, 145−66.
(52) Krause, E., Beyermann, M., Fabian, H., Dathe, M., Rothemund, S., and Bienert, M. (1996) Conformation of a water-soluble β-sheet model peptide: A circular dichroism and Fourier-transform infrared spectroscopic study of double D-amino acid replacements. *Int. J. Pept. Protein Res. 48*, 559−68.
(53) Wu, Y., Huang, H. W., and Olah, G. A. (1990) Method of oriented circular dichroism. *Biophys. J. 57*, 797−806.
(54) Bishop, C. M., Walkenhorst, W. F., and Wimley, W. C. (2001) Folding of β-sheet membrane proteins: Specificity and promiscuity in peptide model systems. *J. Mol. Biol. 309*, 975−88.
(55) Nayar, R., Hope, M. J., and Cullis, P. R. (1989) Generation of large unilamellar vesicles from long-chain saturated phosphatidylcholines by extrusion technique. *Biochim. Biophys. Acta 986*, 200−6.
(56) Ladokhin, A. S., Wimley, W. C., Hristova, K., and White, S. H. (1997) Mechanism of leakage of contents of membrane vesicles determined by fluorescence requenching. *Methods Enzymol. 278*, 474−86.